A New Calibration Method of Three Axis Magnetometer With Nonlinearity Suppression

Hongfeng Pang, Dixiang Chen, Mengchun Pan, Shitu Luo, Qi Zhang, Ji Li, and Feilu Luo

College of Mechatronics Engineering and Automation, National University of Defense Technology, Hunan 410073, China

Nonlinearity is a prominent limitation to the calibration performance of vector magnetometers. A new calibration model is proposed to suppress the nonlinearity of magnetometers and improve calibration performance, in which the nonlinearity coefficients of scale factors are considered. The experimental system mainly consists of a three-axis fluxgate magnetometer (MAG3300), a 2D nonmagnetic rotation equipment, and a proton magnetometer (CZM-3), in which the nonmagnetic rotation equipment is used to change the position of three-axis fluxgate magnetometer, and the scalar value of magnetic field is obtained with the proton magnetometer and considered to be the true value. The principle of this new calibration method is analyzed, and the calibration procedures are introduced. Experimental results show that after nonlinearity suppression, the root-mean-square error of calibration can be reduced by three times. It suggests an effective way to improve the calibration performance of three-axis magnetometers.

***Index Terms*—Nonlinearity, three-axis magnetometer, calibration model, scale factor.**

I. Introduction

THREE-AXIS magnetometers are widely used as magnetic dipole tracking, unexploded ordinance localization, heading sensors of aircraft, and marine vehicles [1]–[4]. The accuracy of three-axis magnetometers is limited by different scales, the bias of each axis, and the nonorthogonality between axes [5], [6]. Therefore, calibration must be performed before the use of three-axis magnetometers.

To calibrate a three-axis magnetometer, calibration parameters should be identified. Merayo *et al.* introduced a linear least squares estimator, which finds the parameters independently and uniquely for a given data [7]. Pylvanainen *et al.* introduced an algorithm that is based on recursive fitting of an ellipsoid [8]. Risbo *et al.* introduced the "thin shell" calibration procedure and developed spherical harmonic modeling, in which a test coil system and an absolute scalar proton magnetometer were utilized [9]. Lotters *et al.* made use of constrained Newton optimization techniques to solve this nonlinear minimization problem directly in the calibration parameter space [10]. Bonnet *et al.* reviewed several approaches and reformulated calibration procedure in an ellipsoid-fitting problem [11]. Gemoz-Egziabher *et al.* introduced a two-step algorithm without external reference based on ellipsoid-fitting. They also used an iterative least-squares estimator to calibrate magnetometer triads, which is initialized using a two-step nonlinear estimator [12], [13]. Foster *et al.* presented an extension of the nonlinear two-step estimation algorithm originally developed for the calibration of solid-state strapdown magnetometers [14]. Vasconcelos *et al.* formulated a maximum likelihood estimator (MLE) to iteratively find the optimal calibration parameters that best fit to the on-board sensor readings, without requiring external attitude [15]. Crassidis *et al.* compared several real-time algorithms for the calibration of three-axis magnetometers performing on-orbit during typical spacecraft mission-mode operations, and unscented Kalman filtering (UKF) algorithm demonstrated better performance [16]. However, magnetometer parameters were considered as constant parameters in the calibration model of traditional methods, and the nonlinearity was ignored. In fact, magnetometer parameters such as scale factors are nonlinear. Nonlinearity is troublesome, which is an important factor influencing the calibration performance of traditional models.

Linearity error was analyzed separately by some researchers. The crossfield effect and hysteresis are two important factors leading to nonlinearity. The crossfield effect or transverse field effect in magnetic sensors is described in literature as an unwanted sensitivity or linearity error due to fields perpendicular to the sensor's sensitive axis [17]. Brauer *et al.* calculated the nonlinearity of the ringcore fluxgate magnetometer due to transverse field [18]. Ripka *et al.* analyzed crossfield effect at fluxgate and tested the racetrack sensor linearity in the presence of transverse and perpendicular fields [19]. Gordon *et al.* presented a fluxgate sensitivity analysis based on a simplified, linearized hysteresis model [20]. Marshall proposed a nonlinear polynomial hysteresis model [21]. Primdahl presented a theoretical analysis of the fluxgate output based on an actual hysteresis curve of a material reproduced by the means of a coordinate measuring table [22]. Some researchers tested and quantitatively analyzed linearity error of fluxgate magnetometers. The linearity error of fluxgate magnetometers may be low in the feedback mode [23]. Kejik *et al.* described the orthogonal fluxgate with flat excitation and pick-up coil, and the linearity error in the 400 mT range is 0.5% [24]. The Oersted fluxgate magnetometer linearity error was below 1 ppm in the earth's field [25]. Hinnrichs *et al.* focused on the noise and linearity of a fluxgate magnetometer in racetrack geometry [26]. Linearity of AMR magnetometers was also analyzed, and linearity of the best present compensated AMR magnetometers is 0.05% [27]. Some researchers proposed a model fitting nonlinearity. The nonlinearity of the sensor is described by the second- to fifth-order coefficients of the spherical harmonic calibration model [28]. Vuillermet *et al.* presented a nonlinear method of moments to predict microfluxgates output [29]. Geiler *et al.* presented a

Manuscript received November 12, 2012; revised January 09, 2013; accepted April 18, 2013. Date of publication April 24, 2013; date of current version August 21, 2013. Corresponding author: H. F. Pang (e-mail: panghongfeng@126.com).

Color versions of one or more of the figures in this paper are available online at http://ieeexplore.ieee.org.

Digital Object Identifier 10.1109/TMAG.2013.2259842

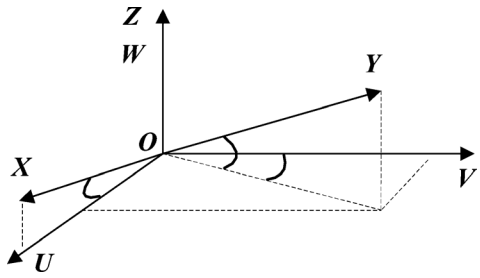

Fig. 1. Orthonormal coordinates and magnetometer coordinates.

quantitative model for the nonlinear response of fluxgate magnetometers [30]. However, nonlinearity was only tested or analyzed separately; little work has been done to solve nonlinearity in vector magnetometer calibration.

In this paper, a new calibration model of three-axis magnetometers is proposed, in which the nonlinearity of magnetometer is considered. Nonlinearity coefficients of scale factors are identified and used to calibrate the magnetometer. The influence of calibration strategy on nonlinearity coefficients is analyzed. The calibration performance of the proposed method outperforms traditional methods. It suggests an effective way to improve the calibration performance of three axis magnetometers.

II. Calibration Method

In order to establish the calibration model of three axis magnetometer, its nonorthogonality error should be analyzed. The relationship between the orthonormal coordinates and three-axis magnetometer coordinates is shown in Fig. 1.

In Fig. 1, O-UVW denotes the orthonormal coordinates and O-XYZ denotes the magnetometer coordinates. The relationship between the two coordinates can be expressed by

$$\begin{bmatrix} u \\ v \\ w \end{bmatrix} = \begin{bmatrix} \cos\alpha & \cos\gamma\sin\beta & 0 \\ 0 & \cos\gamma\cos\beta & 0 \\ \sin\alpha & \sin\gamma & 1 \end{bmatrix} \begin{bmatrix} x \\ y \\ z \end{bmatrix} \tag{1}$$

where α is the angle between the X-axis and the U-axis. γ is the angle between the Y-axis and the UOV-plane. β is the angle between V-axis and the projection of the Y-axis on the UOV-plane. Considering the magnetometer offset and scale factor error in each axis, (1) should be expressed by

$$\begin{bmatrix} B_1 \\ B_2 \\ B_3 \end{bmatrix} = \begin{bmatrix} k_1\cos\alpha & k_2\cos\gamma\sin\beta & 0 \\ 0 & k_2\cos\gamma\cos\beta & 0 \\ k_1\sin\alpha & k_2\sin\gamma & k_3 \end{bmatrix} \begin{bmatrix} B_{m1}-Er_1 \\ B_{m2}-Er_2 \\ B_{m3}-Er_3 \end{bmatrix} \tag{2}$$

where $k_1, k_2,$ and k_3 is the scale factor in X-, Y-, and Z-axis, respectively; $Er_1, Er_2,$ and Er_3 is the offset in X-, Y-, and Z-axis, respectively. $B_m = [B_{m1}, B_{m2}, B_{m3}]^T$ is the measured vector with magnetometer; $B = [B_1, B_2, B_3]^T$ is the true value of magnetic field vector. A further relationship can be obtained by squaring both sides of (2), as follows:

$$\begin{aligned} B^2 = {} & \left(a_{11}^2 + a_{31}^2\right) B_{m1}^2 + \left(a_{12}^2 + a_{22}^2 + a_{32}^2\right) \\ & \times B_{m2}^2 + a_{33}^2 B_{m3}^2 \\ & + 2(a_{11}a_{12} + a_{31}a_{32}) B_{m1}B_{m2} \\ & + 2a_{32}a_{33}B_{m2}B_{m3} + 2a_{31}a_{33}B_{m1}B_{m3} \\ & - 2\left(a_{11}^2 E_{r1} + a_{31}^2 E_{r1} + a_{11}a_{12}E_{r2}\right. \\ & \left. + a_{31}a_{32}E_{r2} + a_{31}a_{33}E_{r3}\right) B_{m1} \\ & - 2\left(a_{11}a_{12}E_{r1} + a_{31}a_{32}E_{r1} + a_{12}^2 E_{r2}\right. \\ & \left. + a_{22}^2 E_{r2} + a_{32}^2 E_{r2} + a_{32}a_{33}E_{r3}\right) B_{m2} \\ & - 2\left(a_{31}a_{33}E_{r1} + a_{32}a_{33}E_{r2} + a_{33}^2 E_{r3}\right) B_{m3} \\ & + f(E_{r1}, E_{r2}, E_{r3}) \end{aligned} \tag{3}$$

where

$$\begin{aligned} a_{11} &= k_1\cos\alpha \\ a_{12} &= k_2\sin\beta\cos\gamma \\ a_{22} &= k_2\cos\beta\cos\gamma \\ a_{31} &= k_1\sin\alpha \\ a_{32} &= k_2\sin\gamma \\ a_{33} &= k_3. \end{aligned} \tag{4}$$

Equation (3) can be expressed by

$$\begin{aligned} B^2 = {} & P_1 B_{m1}^2 + P_2 B_{m2}^2 + P_3 B_{m3}^2 \\ & + P_4 B_{m1}B_{m2} + P_5 B_{m2}B_{m3} \\ & + P_6 B_{m1}B_{m3} + P_7 B_{m1} \\ & + P_8 B_{m2} + P_9 B_{m3} + P_{10} \end{aligned} \tag{5}$$

where $P_1, \ldots, P_9$ are functions of parameters $k_1, k_2, k_3, \alpha, \beta, \gamma, P_{10} = f(E_{r1}, E_{r2}, E_{r3})$ is the function of E_{r1}, E_{r2}, E_{r3}.

The magnetometer parameters $k_1, k_2, k_3, \alpha, \beta, \gamma, Er_1, Er_2, Er_3$ can be computed when $P_1, \ldots, P_{10}$ are known. The details of conventional magnetometer calibration can be found in [7]. The third-order nonlinearity coefficients should be considered [28]. When considering the nonlinearity of scale factor in each axis, (4) can be expressed by

$$\begin{aligned} a_{11} &= \left(k_{x0} + k_{x1}B_{m1} + k_{x2}B_{m1}^2 + k_{x3}B_{m1}^3\right) \\ &\quad \times \cos\alpha \\ a_{12} &= \left(k_{y0} + k_{y1}B_{m2} + k_{y2}B_{m2}^2 + k_{y3}B_{m2}^3\right) \\ &\quad \times \sin\beta\cos\gamma \\ a_{22} &= \left(k_{y0} + k_{y1}B_{m2} + k_{y2}B_{m2}^2 + k_{y3}B_{m2}^3\right) \\ &\quad \times \cos\beta\cos\gamma \\ a_{31} &= \left(k_{x0} + k_{x1}B_{m1} + k_{x2}B_{m1}^2 + k_{x3}B_{m1}^3\right) \\ &\quad \times \sin\alpha \\ a_{32} &= \left(k_{y0} + k_{y1}B_{m2} + k_{y2}B_{m2}^2 + k_{y3}B_{m2}^3\right) \\ &\quad \times \sin\gamma \\ a_{33} &= \left(k_{z0} + k_{z1}B_{m3} + k_{z2}B_{m3}^2 + k_{z3}B_{m3}^3\right) \end{aligned} \tag{6}$$

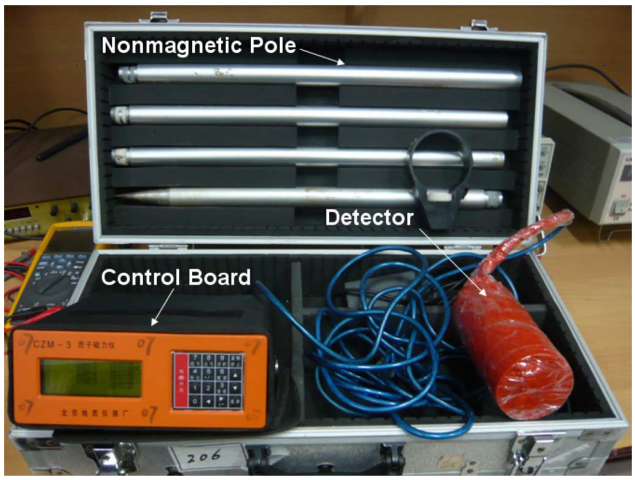

Fig. 2. Proton magnetometer.

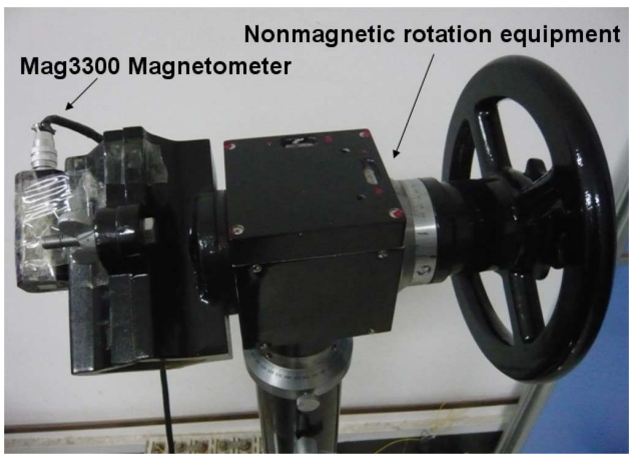

Fig. 3. Mag3300 magnetometer and nonmagnetic rotation equipment.

where k_{x0}, k_{y0}, and k_{z0} is the constant coefficient of scale factor in the X-, Y-, and Z-axis, respectively. k_{x1}, k_{y1}, and k_{z1} is the first-order nonlinearity coefficient of scale factor in X-, Y-, and Z-axis, respectively. k_{x2}, k_{y2}, and k_{z2} is the second-order nonlinearity coefficient of scale factor in X-, Y-, and Z-axis respectively. k_{x3}, k_{y3}, and k_{z3} is the third-order nonlinearity coefficient of scale factor in X-, Y-, and Z-axis, respectively.

These magnetometer parameters $k_{x0}, k_{y0}, k_{z0}, k_{x1}, k_{y1}, k_{z1}, k_{x2}, k_{y2}, k_{z2}, k_{x3}, k_{y3}, k_{z3}, \alpha, \beta, \gamma, Er_1, Er_2$, and Er_3 can be computed by solving nonlinear equations when a group of magnetometer measurements are known. It is shown that at least 18 datasets should be measured because there are 18 magnetometer parameters, and the least square method can be used when more data are measured. Thus, three-axis magnetometers can be calibrated with the calibration model:

$$\begin{bmatrix} B_1 \\ B_2 \\ B_3 \end{bmatrix} = \begin{bmatrix} a_{11} & a_{12} & 0 \\ 0 & a_{22} & 0 \\ a_{31} & a_{32} & a_{33} \end{bmatrix} \begin{bmatrix} B_{m1} - Er_1 \\ B_{m2} - Er_2 \\ B_{m3} - Er_3 \end{bmatrix}. \quad (7)$$

III. Experiments

A. Experimental System

The experimental system consists of a CZM-3 proton magnetometer (to provide the true scalar value of magnetic field, shown in Fig. 2), a MAG3300 three-axis fluxgate magnetometer (to be calibrated, shown in Fig. 3), a two-dimensional nonmagnetic rotation equipment (to change the position of three-axis fluxgate magnetometer, shown in Fig. 3), a notebook computer (to record and save measurement results), data acquisition software (program with C++ Builder), and data processing software (program with Matlab 7.1).

The main performance specifications of MAG3300 fluxgate magnetometer are listed as follows:

- field range of each axis: $\pm 100\,000$ nT;
- resolution: 1 nT;
- orthogonality error: $< \pm 0.5^\circ$;
- bias tested in nonmagnetic shield equipment: $< \pm 1000$ nT;

The main performance specifications of CZM-3 proton magnetometer are listed as follows:

- field range: 30 000 nT to 70 000 nT (scalar value);
- resolution: 0.1 nT;
- accuracy: ± 1 nT.

B. Experimental Procedure

1) A site with little magnetic disturbance is chosen to be the calibration position. The magnetic field of the Earth was used in the experiments, and the proton magnetometer is used to measure the true scalar value of magnetic field. The three-axis fluxgate magnetometer is fixed on the nonmagnetic rotation equipment to obtain measurements with different positions. The sampling rate is 20 Hz. Two groups of data are obtained with different measurement strategies.

2) The first group of data is obtained with symmetrical measurement strategy. First, both horizontal rotation angle and upright rotation angle of the 2D nonmagnetic rotation equipment are adjusted to be zero, and the magnetic field vector is measured with three-axis magnetometer about one minute, and the average is considered as measured value, which is helpful to reduce the measurement error and suppress ambient noise. Second, the horizontal rotation angle is fixed, and the upright rotation angle is increased by 60°, and the magnetic field vector is measured in the same way. Then, the horizontal rotation angle is increased by 60° when the upright rotation angle became 360° (0°). The above steps are repeated until 36 measured vectors are obtained. In this strategy, magnetometer position distributes uniformly in 3D.

3) The second group of data is obtained with random measurement strategy. The three-axis magnetometer is rotated randomly and continuously using the nonmagnetic rotation equipment. "Randomly and continuously" means that the three-axis magnetometer is rotated continuously, and the rotation direction is random. Because it takes less time to adjust the position of magnetometer in this strategy, more measurements can be acquired in the same time.

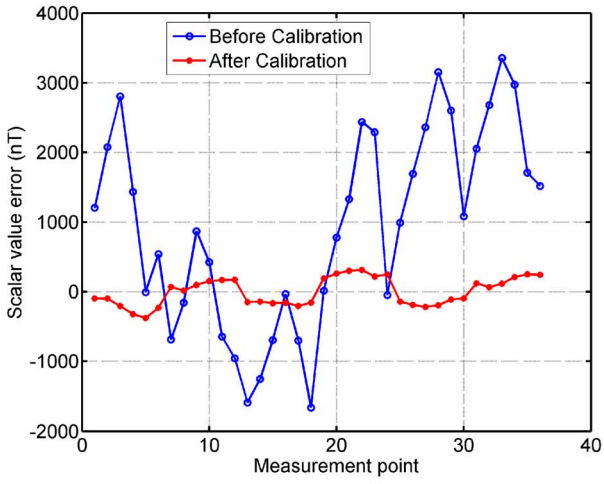

Fig. 4. Calibration result of the first group of data without nonlinearity suppression.

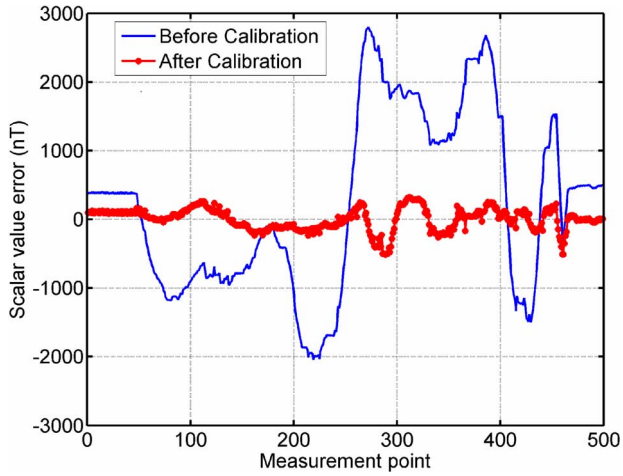

Fig. 6. Calibration result of the second group of data without nonlinearity suppression.

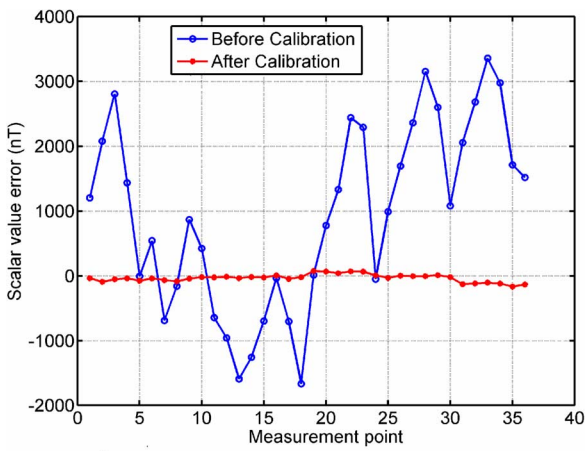

Fig. 5. Calibration result of the first group of data with nonlinearity suppression.

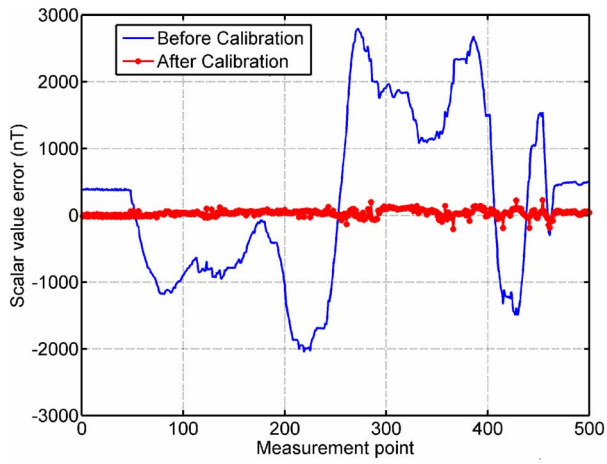

Fig. 7. Calibration result of the second group of data with nonlinearity suppression.

IV. Calibration Results

A. Calibration Result of the First Group of Data

In order to evaluate the calibration performance, the RMS error of magnetic field intensity is analyzed, which is defined by

$$\sigma = \sqrt{\frac{1}{N-1}\sum_{k=1}^{N}\left(\sqrt{(B_k^x)^2+(B_k^y)^2+(B_k^z)^2}-B_{\text{true}}\right)^2} \tag{8}$$

where B_k^x, B_k^y, and B_k^z are the three components of the measured vector, and B_{true} is the true scalar value. N is the number of measured data. Fig. 4 shows the calibration result without nonlinearity suppression, in which the first group of data is used (contains 36 measurements). After calibration, the root mean square (RMS) error of scalar value is reduced from 1725.059 to 198.855 nT. Fig. 5 shows the calibration result with nonlinearity suppression. Comparing Fig. 5 with Fig. 4, it is obvious that the calibration performance is improved. After calibration with nonlinearity suppression, the RMS error of scalar value is reduced to 68.152 nT, which is 34.27% of the calibration error without nonlinearity suppression.

B. Calibration Result of the Second Group of Data

Fig. 6 shows the calibration result without nonlinearity suppression, in which the second group of data is used (contains 500 measurements). After calibration, the RMS error of scalar value is reduced from 1312.549 to 171.814 nT. Fig. 7 shows the calibration result with nonlinearity suppression. Comparing Fig. 7 with Fig. 6, it is obvious that the calibration performance is improved. After calibration with nonlinearity suppression, the RMS error of scalar value is reduced to 59.846 nT (34.84%), which is also much less than the calibration error without nonlinearity suppression. Compared with the two groups of data, it is similar that the RMS error of scalar value is reduced to 1/3 after calibration with nonlinearity suppression.

V. Discussion

Table I shows that the estimated nonlinearity coefficients of scale factors, and nonlinearity coefficients of

TABLE I
ESTIMATED PARAMETERS OF THE MAG3300 MAGNETOMETER

k_{x0}	k_{x1}	k_{x2}	k_{x3}	k_{y0}	k_{y1}
0.9668	-4.9e-9	-9.8e-14	4.1e-23	0.9813	6.9e-9
k_{y2}	k_{y3}	k_{z0}	k_{z1}	k_{z2}	k_{z3}
4.1e-14	-1.1e-23	1.0036	1.5e-6	4.5e-14	2.5e-22
α	β	γ	Er_1	Er_2	Er_3
-0.06628	-0.01718	-0.25009	-1009.3	-799.2	-829.7

X-, Y-, and Z-axis are similar. It also shows the estimated nonorthogonality error and bias of each axis. It is clear that the northogonal errors are less than 0.05°, which are in the range of specifications. In addition, the bias of each axis is similar. In fact, the Mag3300 magnetometer has been used for several years, so the circuit characteristic has changed to some extent.

The magnetometer error was reduced from 1840.8 to 93.1 nT in [14]. As shown in Figs. 5 and 7, there are residual errors after calibration, even if error is reduced about 25 times. This is because magnetometer hysteresis, temperature error, and noise have not been completely solved. In addition, in order to further improve the calibration performance, a more desired calibration place should be considered, for example, a geomagnetic observatory station.

VI. CONCLUSION

Nonlinearity is a prominent limitation to the calibration performance of three axis magnetometers, which is ignored in traditional calibration methods. In this paper, a new calibration model considering the nonlinearity coefficients of magnetometer is proposed. After calibration with the proposed method, the RMS error can be reduced to one third of the scalar error without nonlinearity suppression. The experiments indicate that the influence of measurement strategy during the calibration is not obvious. It suggests an effective method to improve the calibration performance of three-axis magnetometers.

ACKNOWLEDGMENT

This research is sponsored by National Natural Science Foundation of China (project number: 51175507). The authors would like to extend their appreciation to magnetism laboratory of CSIC-No.710 research institute for their contributions to the work.

REFERENCES

[1] W. Yang, C. Hu, M. Q. H. Meng, S. Song, and H. Dai, "A six-dimensional magnetic localization algorithm for rectangular magnet objective based on a particle swarm optimizer," *IEEE Trans. Magn.*, vol. 45, no. 8, pp. 3092–3099, Aug. 2009.

[2] A. Sheinker, L. Frumkis, B. Ginzburg, N. Salomonski, and B.-Z. Kaplan, "Magnetic anomaly detection using a three-Axis magnetometer," *IEEE Trans. Magn.*, vol. 45, no. 1, pp. 160–167, Jan. 2009.

[3] J. Včelák, P. Ripka, J. Kubik, A. Platil, and P. Kaspar, "AMR navigation systems and methods of their calibration," *Sens. Actuators A*, vol. 123, pp. 122–128, 2005.

[4] M. Birsan, "Recursive Bayesian method for magnetic dipole tracking with a tensor gradiometer," *IEEE Trans. Magn.*, vol. 47, no. 2, pp. 409–415, Feb. 2011.

[5] H. Auster, K. Fornacon, E. Georgescu, K. Glassmeier, and U. Motschmann, "Calibration of fluxgate magnetometers using relative motion," *Meas. Sci. Technol.*, vol. 13, pp. 1124–1131, 2002.

[6] W. Koo, S. Sung, and Y. Lee, "Error calibration of magnetometer using nonlinear integrated filter model with inertial sensors," *IEEE Trans. Magn.*, vol. 45, no. 6, pp. 2740–2743, 2009.

[7] J. Merayo, P. Brauer, F. Primdahl, J. Petersen, and O. Nielsen, "Scalar calibration of vector magnetometers," *Meas. Sci. Technol.*, vol. 11, pp. 120–132, 2000.

[8] T. Pylvanainen, "Automatic and adaptive calibration of 3D field sensors," *Appl. Math. Model.*, vol. 32, pp. 575–587, 2007.

[9] T. Risbo, P. Brauer, J. Merayo, O. Nielsen, J. Petersen, F. Primdahl, and I. Richter, "Ørsted pre-flight magnetometer calibration mission," *Meas. Sci. Technol.*, vol. 14, pp. 674–688, 2003.

[10] J. Lotters, J. Schipper, P. Veltink, W. Olthuis, and P. Bergveld, "Procedure for in-use calibration of triaxial accelerometers in medical applications," *Sens. Actuators A*, vol. 68, pp. 221–228, 1998.

[11] S. Bonnet, C. Bassompierre, C. Godin, S. Lesecq, and A. Barraud, "Calibration methods for inertial and magnetic sensors," *Sens. Actuators A*, vol. 156, pp. 302–311, 2009.

[12] D. Gemoz-Egziabher, G. Elkaim, D. Powell, and B. Parkinson, "Calibration of strap-down magnetometers in magnetic field domain," *J. Aerosp. Eng.*, vol. 19, pp. 87–102, 2006.

[13] D. Gemoz-Egziabher, "Magnetometer autocalibration leveraging measurement locus constraints," *J. Aircraft.*, vol. 44, pp. 1361–1368, 2007.

[14] C. Foster and G. Elkaim, "Extension of a two-step calibration methodology to include nonorthogonal sensor axes," *IEEE Trans. Aerosp. Electron. Syst.*, vol. 44, no. 3, pp. 1070–1078, 2008.

[15] J. Vasconcelos, G. Elkaim, C. Silvestre, P. Oliveira, and B. Cardeira, "Geometric approach to strapdown magnetometer calibration in sensor frame," *IEEE Trans. Aerosp. Electron. Syst.*, vol. 47, no. 2, pp. 1293–1306, 2011.

[16] J. Crassidis, K. Lai, and R. Harman, "Real-time attitude-independent three-axis magnetometer calibration," *J. Guid. Control Dynam.*, vol. 28, pp. 115–120, 2005.

[17] M. Janosek, M. Butta, and P. Ripka, "Two sources of cross-field error in racetrack fluxgate," *J. Appl. Phys.*, vol. 107, pp. 09E7131–09E7133, 2010.

[18] P. Brauer, J. Merayo, O. Nielsen, F. Primdahl, and J. Petersen, "Transverse field effect in fluxgate sensors," *Sens. Actuators A*, vol. 59, pp. 70–74, 1997.

[19] P. Ripka and S. Billingsley, "Crossfield effect at fluxgate," *Sens. Actuators A*, vol. 81, pp. 176–179, 2000.

[20] D. Gordon, R. Ludsten, and R. Chiarodo, "Factors affecting the sensitivity of gamma-level ring-core magnetometers," *IEEE Trans. Magn.*, vol. 1, no. 4, pp. 330–337, 1965.

[21] S. Marshall, "An analytic model for the fluxgate magnetometer," *IEEE Trans. Magn.*, vol. 3, no. 3, pp. 459–463, 1967.

[22] F. Primdahl, "The fluxgate mechanism, part 1: The gating curves of parallel and orthogonal fluxgates," *IEEE Trans. Magn.*, vol. 6, no. 2, pp. 376–383, 1970.

[23] O. Nielsen, J. Petersen, F. Primdahl, P. Brauer, B. Hernando, A. Fernandez, J. Merayo, and P. Ripka, "Development, construction and analysis of the 'Oersted' fluxgate magnetometer," *Meas. Sci. Technol.*, vol. 6, pp. 1099–1115, 1995.

[24] P. Kejik, L. Chiesi, B. Ianossy, and R. Popovic, "A new compact 2D planar fluxgate sensor amorphous metal core," *Sens. Actuators A*, vol. 81, pp. 180–183, 2000.

[25] O. Nielsen *et al.*, "A high-precision triaxial fluxgate sensor for space applications: layout and choice of materials," *Sens. Actuators A*, vol. 59, pp. 168–176, 1997.

[26] C. Hinnrichs, C. Pels, and H. Schilling, "Noise and linearity of a fluxgate magnetometer in racetrack geometry," *J. Appl. Phys.*, vol. 87, pp. 7085–7087, 2000.

[27] P. Ripka, M. Vopálenský, A. Platil, M. Döscher, K. Lenssen, and H. Hauser, "AMR magnetometer," *J. Magn. Magn. Mater.*, vol. 254, pp. 639–641, 2003.

[28] P. Brauer, T. Risbo, J. Merayo, and O. Nielsen, "Fluxgate sensor for the vector magnetometer on board the 'Astrid-2' satellite," *Sens. Actuators A*, vol. 81, pp. 184–188, 2000.

[29] Y. Vuillermet, M. Audoin, and R. Cuche, "Application of a non-linear method of moments to predict microfluxgates output," *Sens. Actuators A*, vol. 158, pp. 212–216, 2010.

[30] A. Geiler, V. Harris, C. Vittoria, and N. Sun, "A quantitative model for the nonlinear response of fluxgate magnetometers," *J. Appl. Phys.*, vol. 99, pp. 08B3161–08B3163, 2006.